Molecular Heterogeneity of a Type III Cytotoxin, *Pseudomonas aeruginosa* Exoenzyme S†

Anthony W. Maresso, Matthew J. Riese, and Joseph T. Barbieri*

Microbiology and Molecular Genetics, Medical College of Wisconsin, 8701 Watertown Plank Road, Milwaukee, Wisconsin 53226

Received June 18, 2003; Revised Manuscript Received September 29, 2003

ABSTRACT: *Pseudomonas aeruginosa* ExoS is a bifunctional type III cytotoxin. The N-terminus (residues 1−232) is a Rho GTPase activating protein (GAP) domain, while the C-terminus (residues 233−453) is a FAS-dependent ADP-ribosyltransferase domain that targets Ras and Ras-like GTPases. A membrane localization domain (residues 51−72) localizes ExoS to a perinuclear region within eukaryotic cells. Recent studies observed that ExoS is auto-ADP-ribosylated upon delivery into eukaryotic cells. Auto-ADP-ribosylated ExoS analyzed from eukaryotic cells displayed p*I* heterogeneity and prompted an analysis of this heterogeneity. Bacterial-associated ExoS and ExoS that had been secreted by *P. aeruginosa* also showed p*I* heterogeneity with five charge forms ranging in p*I* from 5.1 to 5.9. The p*I* heterogeneity of ExoS was independent of a mass change and thus represented molecular charge conformers. Urea was not required to observe the p*I* conformers of ExoS; it enhanced the resolution and formation of p*I* conformers during the focusing component of the analysis. ExoS(E381D), a mutant deficient in ADP-ribosyltransferase activity, isolated from cultured cells showed charge forms that migrated to a more acidic p*I* than type III secreted ExoS but more basic than auto-ADP-ribosylated ExoS. Incubation of cell lysates with Mn^{2+} shifted the p*I* of ExoS(E381D) to a p*I* identical to secreted ExoS. This indicates that within the mammalian cells ExoS undergoes a negatively charged modification, in addition to auto-ADP-ribosylation observed for wild-type ExoS. ExoT, ExoU, and YopE also focus into multiple p*I* forms, suggesting that this is a common property of type III cytotoxins.

Pseudomonas aeruginosa is a Gram-negative opportunistic pathogen that infects burn victims, cystic fibrosis patients, and the immunocompromised (*1*). Several virulence determinants, both cell-associated and secreted, contribute to the pathogenesis of *P. aeruginosa*. Four of these determinants, ExoS,[1] ExoT, ExoU, and ExoY, are type III cytotoxins delivered directly into the eukaryotic cell by the bacterium. ExoS is a 453 amino acid, bifunctional protein. The N-terminus (residues 1−232) is a Rho GAP domain (*2*) while the C-terminus (residues 233−453) is a FAS-dependent ADP-ribosyltransferase domain (*3*, *4*). The ADP-ribosyltransferase activity covalently attaches an ADP-ribose moiety from NAD onto several host proteins, including Ras GTPases. Glutamic acid 381 is an ADP-ribosyltransferase active site residue of ExoS, and forms of ExoS that contain mutations in this residue are useful for exploring the role of ADP-ribosylation in ExoS-mediated cytotoxicity (*5*−*8*). A membrane localization domain (residues 51−72, MLD) localizes ExoS to a perinuclear region within eukaryotic cells. Deletion of the MLD eliminated the ability of ExoS to ADP-ribosylate Ras in vivo, but not in vitro, indicating the MLD contributes to Ras targeting inside eukaryotic cells (*9*). Deletion of the MLD allows for the purification of ExoS, ExoSΔ51−72, to homogeneity (*10*), facilitating biochemical and biophysical analysis.

The type III secretion system (TTSS) of *P. aeruginosa* is a virulence determinant during infection (*11*). The TTSS is composed of more than 20 proteins (*12*, *13*) that transport ExoS from the bacterial cytoplasm (bacterial intracellular ExoS) through the outer membrane (secreted ExoS). In many Gram-negative bacteria, acidic chaperone proteins aid in the secretion of type III cytotoxins (*14*, *15*). Deletion of chaperones leads to degradation or aggregation of their cognate type III cytotoxin (*16*). The transport of type III cytotoxins through the TTSS requires a secretion signal. The nature of this signal remains controversial but may reside in the mRNA (*17*) or N-terminal polypeptides of the type III cytotoxin (*18*). In *P. aeruginosa*, PopB, PopD, and PcrV are implicated to form a pore to deliver ExoS (translocated ExoS) into the eukaryotic cell (*19*, *20*).

Recent studies observed that ExoS is auto-ADP-ribosylated upon type III translocation into eukaryotic cells (*21*). During experiments to characterize the auto-ADP-ribosylation of ExoS, 2D SDS−PAGE showed that ExoS focused as multiple p*I* forms. This study characterizes the molecular basis for the multiple charge forms of ExoS.

EXPERIMENTAL PROCEDURES

Protein Purification and Preparation. The deletion protein ExoS(232−453) was purified from *Escherichia coli* [pET15b-

† This work was supported by grants from the National Institutes of Health (HL68912 and AI30162).

* Corresponding author. Phone: 414-456-8412. Fax: 414-456-6536. E-mail: jtb01@mcw.edu.

[1] Abbreviations: ExoS, exoenzyme S; ADPr, adenosine diphosphate ribosyltransferase; FAS, factor activating ExoS; GAP, GTPase activating protein.

10.1021/bi035053i CCC: $25.00
Published on Web 11/13/2003

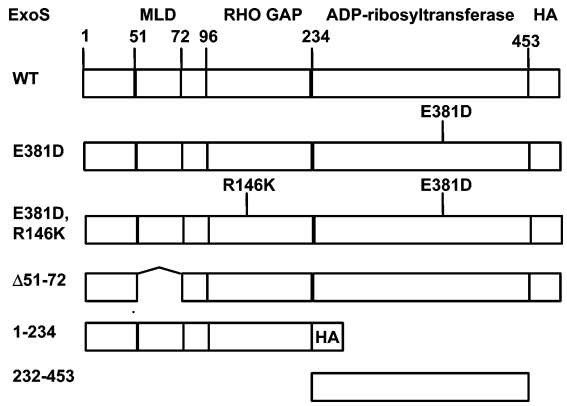

FIGURE 1: Schematic representation of ExoS constructs and domains. ExoS consists of a membrane localization domain (MLD, 51−72), an N-terminal GAP domain (96−234), and a C-terminal ADP-ribosyltransferase domain (232−453). Proteins were HA-tagged (see Experimental Procedures) to facilitate analysis by Western blot.

ExoS(232−453)] as previously described (*22*). Three forms of ExoS were subjected to analysis: bacterial intracellular ExoS, secreted ExoS, and eukaryotic intracellular ExoS.

(A) Isolation of Secreted ExoS. Purification of secreted forms of ExoS from *P. aeruginosa* has been described (*23*). Briefly, *P. aeruginosa* pUCP-ExoS-HA (*21*), pUCP-ExoS-(E381D)-HA, pUCP-ExoS(Δ51−72)-HA, or pUCP-ExoS-(1−234)-HA (*9*) (Figure 1) was cultured at 30 °C (200 rpm) in 20 mL of secretion media. At $A_{540} = 4$, the culture medium was centrifuged at 8000*g* for 20 min. The supernatant was passed through a 0.45 μm filter and subjected to ammonium sulfate precipitation (final concentration = 60%) at 4 °C for 12 h. The suspension was centrifuged at 16000*g* for 20 min, and the precipitated material was suspended in 10 mM Tris and 20 mM NaCl (pH 7.6). Solubilized proteins were subjected to Sephacryl-200 gel filtration (450 mL, 10 mM Tris, 20 mM NaCl (pH 7.6), 0.4 mL/min at 4 °C), and 3.5 mL fractions were collected. Peak fractions were pooled and designated "secreted ExoS". The concentration of secreted ExoS was determined by comparison to a BSA standard using SDS−PAGE, assuming equimolar staining for Coomassie blue. ExoT and ExoU were isolated from culture supernatants of *P. aeruginosa* as previously described (*24*, *25*). Isolation of YopE from culture supernatants of *P. aeruginosa* was performed essentially as above for ExoS.

(B) Isolation of Bacterial Intracellular ExoS. Bacterial intracellular ExoS-HA and ExoS(E381D)-HA were isolated from cultured *P. aeruginosa* as follows: after centrifugation pelleted bacteria were suspended in 5 mL of 5 mM Tris-HCl (pH 7.6) and passed three times through a French press. Lysed cultures were centrifuged at 16000*g* for 45 min, and the soluble material was passed through a 0.45 μm filter. This material contained "bacterial intracellular ExoS", which was subjected to isoelectric focusing followed by SDS−PAGE. Total protein concentrations were determined with a BCA reagent kit (Pierce, Rockford, IL), using BSA as a standard. Bacterial intracellular ExoS concentrations were determined by Western analysis using known concentrations of purified ExoSΔ51−72-HA.

(C) Isolation of Eukaryotic Intracellular ExoS: Infection. Confluent lawns of CHO cells (85 mm dish cultures incubated in F12 media containing 10% newborn calf serum, 0.1% $NaHCO_3$ Penn/Strep, and 5% CO_2) were infected with *P. aeruginosa* pUCP-ExoS-HA or pUCP-ExoS(E381D)-HA at an MOI of 8:1 (bacteria:CHO cells) at 37 °C. *P. aeruginosa* were quantified from the absorbance calculation $1A_{540} = 4 \times 10^8$ bacteria. At confluent growth, there are ~4×10^6 CHO cells in an 85 mm dish. After a 4 h infection, cells were washed with PBS and incubated with F12 media, supplemented with gentamycin (0.4 mg/mL) and ciprofloxacin (0.7 mg/mL) for 1 h. This 1 h incubation allowed delivery of bacterial-associated ExoS into the eukaryotic cell as measured by the extent of cell-associated ExoS that was auto-ADP-ribosylated (M. J. Riese and J. T. Barbieri, unpublished data). CHO cells were washed with PBS, scraped, centrifuged at 3000*g* for 5 min, and suspended in 150 μL of lysis buffer [10 mM Tris, pH 7.6, containing 0.5 mM EDTA, 250 mM sucrose, 3 mM imidazole, and a 1:100 dilution of mammalian protease inhibitor cocktail (Sigma, P8340)]. Addition of this protease cocktail prevented degradation of ExoS during 2D SDS−PAGE (A. W. Maresso and J. T. Barbieri, unpublished data). CHO cells were broken by passage (20 times) through a $^5/_8$ in. 22-gauge needle. CHO cell lysates were centrifuged at 3000*g* for 10 min, and the postnuclear supernatants (PNS) were precipitated with acetone (final concentration = 90%) for 2 h. The precipitated material was collected by centrifugation at 13000*g* for 10 min and suspended in IEF buffer [8 M urea, 10% CHAPS, 0.1% DTT, 0.5% carrier ampholytes, pH 4−7 (Pharmacia, Uppsala, Sweden), and a 1:100 dilution of the mammalian protease inhibitor cocktail (Sigma)].

(D) Transfection. pEGFP-N1-ExoS(R146K,E381D)-HA was engineered as follows: pUCP-ExoS[1−234(R146K)] (*2*, *26*) was digested with *Eag*I/*Bam*HI and ligated with the *Eag*I/*Bam*HI fragment of pUCP-ExoS(E381D)-HA to create pUCP-ExoS(R146K,E381D)-HA. pUCP-ExoS(R146K,-E381D)-HA was digested with *Hin*dIII and *Bam*HI to remove the DNA encoding ExoS[1−453(R146K,E381D)]-HA, and this fragment was subcloned into the *Hin*dIII/*Bam*HI sites of pEGFP-N1 (Clonetech) to create pEGFP-N1-ExoS-(R146K,E381D)-HA. This construct encodes a stop codon 3′ to the HA tag. Three micrograms of DNA encoding pEGFP-N1-ExoS(R146K,E381D)-HA was transiently cotransfected (Lipofectamine Plus, Invitrogen) with 1.2 μg of the pEGFP-N1 vector into 70% confluent CHO cells (85 mm dish cultures in complete F12 media with 5% CO_2) according to manufacturer's instructions. Eighteen hours posttransfection, postnuclear supernatants were harvested as described for infected ExoS.

2D SDS−PAGE. IEF was performed in a Protean IEF cell (Bio-Rad) using 7 cm (pH 4−7) linear strips (Pharmacia). Focusing parameters were as follows: strips were passively hydrated with 125 μL of IEF buffer plus sample for 12 h. Maximum μA/gel = 50; step 1 = 500 V for 250 V h, step 2 = 1000 V for 500 V h, step 3 = 8000 V for 8000 V h, and step 4 = 500 V (hold). Typically, 50−500 ng of secreted, bacterial, or eukaryotic intracellular ExoS-HA, ExoS(E381D)-HA, ExoS(R146K,E381D)-HA, ExoS(Δ51−72)-HA, ExoS-(1−234)-HA, or ExoS(232−453) was focused. Following IEF, strips were incubated for 15 min in SDS equilibration buffer [50 mM Tris-HCl (pH 8.6) containing 6 M urea, 30% glycerol, 2% SDS, trace amounts of bromophenol blue, and 25 mg/mL iodoacetamide], followed by a 15 min incubation in SDS equilibration buffer containing 10 mg/mL dithiothreitol. Strips were added directly to 10% or 13.5% SDS−

PAGE gels and electrophoresed at 15 mA. Either the gels were stained with Coomassie blue or silver (*27*) or proteins were transferred to PVDF membranes and probed with mouse α-HA monoclonal IgG (Babco, Princeton, NJ, at a 1:3000 dilution) for 1 h at room temperature and then goat α-mouse IgG conjugated to HRP (Pierce at a 1:45000 dilution) for 1 h at room temperature. For mixing experiments, 50 ng of the indicated forms of ExoS was mixed and added to the IEF system. For the p*I* shift experiments, transfected ExoS(R146K,E381D) in postnuclear supernatants was incubated with ExoS(E381D) secreted from *P. aeruginosa* alone or with WT ExoS (isolated from infection assays) in either the presence (0.5 mM) or absence of $MnCl_2$. Reaction volumes were adjusted to 20 μL with H_2O, and incubations were for 30 min at 37 °C. The p*I* of ExoS spots was determined by comparison to the position of p*I* standards (Bio-Rad, p*I* 4.5−8.5 standards) mixed with ExoS proteins during the same IEF run. Two-dimensional gels were analyzed using Phoretix 2D software (Nonlinear Dynamics).

Molecular Sizing of ExoSΔ51−72. For analytical ultracentrifugation, 100 μL of ExoSΔ51−72 from *E. coli* (280 nm absorbances of 0.8, 0.5, and 0.2) was subjected to sedimentation equilibrium. Runs were performed at 4 °C for 72 h, and absorbance was measured against a reference dialysate. Data were monitored by measuring the log of the absorbance vs the radial position (from a reference cell) and modeled as a monomer. The buffer specific density was 1.005343 g/mL, the partial specific volume was 0.729 mL/g, and the extinction coefficient was 18910 M^{-1} cm^{-1}.

MALDI-TOF Mass Spectrometry. ExoSΔ51−72 secreted and gel filtration purified from *P. aeruginosa* was subjected to IEF as described above. The 5.1, 5.3, 5.5, 5.7, and 5.9 p*I* forms were excised from Coomassie-stained 13.5% SDS−PAGE gels, sonicated three times in a water bath sonicator for 5 min in 400 μL of 50% acetonitrile (H_2O), and placed in the appropriate protease buffer. The reactions were as follows: trypsin (Promega, Madison, WI) and V8 protease (Pierce) at 0.02 μg/μL in 50 μL of 100 mM NH_4HCO_3 (pH 8); submaxillaris protease (Pierce) at 0.02 μg/μL in 50 μL of 1% $NaHCO_3$ (pH 8). Incubations were at 37 °C for 24 h. Following digestion, gel slices were sonicated two times in 200 μL of 80% acetonitrile and 1% formic acid (in H_2O) for 10 min. Washes were combined and evaporated by speed vacuum centrifugation, and the pellet was dissolved in 15 μL of 0.1% trifluoroacetic acid (TFA) (H_2O). C18 Zip Tips (Millipore, Bedford, MA) were equilibrated successively in 15 μL of 100% acetonitrile, 15 μL of 50% acetonitrile (H_2O), and 15 μL of 0.1% TFA (H_2O) prior to addition of peptides. Peptides were bound to the resin, washed twice with 0.1% TFA in H_2O, eluted with 2 μL of 60% acetonitrile and 0.1% TFA (H_2O saturated with α-cyano-4-hydroxycinnamic acid), and applied to a sample plate to air-dry. Samples were ionized by a N_2 UV laser using a PE-pro mass spectrometer (Applied Biosystems). Two hundred laser shots were conducted at an accelerating voltage of 25000 V and laser intensity of 2075 (repetition rate 3 Hz). Scans were processed using Biosystems Voyager 6004 software.

2D SDS−PAGE of pI Forms of ExoS. Elution of the 5.3, 5.5, and 5.7 p*I* forms of ExoS from Coomassie-stained 13.5% SDS−PAGE gels was achieved by modification of a protocol for elution of proteins from SDS−PAGE gels (*28*). Briefly, 50 μg of ExoSΔ51−72 secreted and purified for *P. aeruginosa* was subjected to 2D SDS−PAGE with the following IEF modifications: 18 cm, pH 4−7 linear strips were utilized. Step 1 = 500 V for 1 V h, step 2 = 3500 V for 3000 V h, step 3 = 3500 V for 20000−27000 V h, and step 4 at 500 V (hold). The IEF strip was then subjected to SDS−PAGE, and proteins were identified by Coomassie staining. The gel was destained in H_2O, the 5.3, 5.5, and 5.7 p*I* forms of ExoS were excised, and the gel was ground to minute pieces with a 200 μL pipet tip. IEF buffer (125 μL) was added, and the gel pieces were sonicated in a water bath sonicator for 30 min. After sonication, the gel pieces/IEF buffer mixture was subjected to 2D SDS−PAGE using pH 4−7 (linear, 7 cm) IEF focusing as described above.

ADP-Ribosyltransferase Activity. A linear velocity reaction was employed to determine the trans and auto-ADP-ribosyltransferase activity of ExoSΔ51−72 toward ExoSΔ51−72 and soybean trypsin inhibitor (SBTI), respectively (*10*). Briefly, the ExoSΔ51−72 5.5 p*I* form (45 nM), eluted from an SDS−PAGE gel (see above), and uneluted ExoSΔ51−72 (purified from *P. aeruginosa*) were incubated in a 20 μL reaction with [^{32}P]NAD (specific activity 250 Ci/mmol), SBTI (5 μM), and FAS (250 nM) in 0.3 M urea and 0.5% CHAPS for 1, 2, or 4 min. Reactions were quenched with the addition of SDS−PAGE sample buffer [8% SDS, 0.1% bromophenol blue, 80% glycerol, 2.5% βME, and 75 mM Tris-HCl (pH 7.6)], boiled for 5 min, and applied to 13.5% SDS−PAGE. Coomassie-stained SBTI and ExoSΔ51−72 bands were exposed to autoradiography, excised, and subjected to scintillation analysis. For autoribosylation of ExoSΔ51−72, SBTI was emitted from the reactions. Protein concentrations were determined by creation of a standard curve with known amounts of BSA, assuming that these proteins had equimolar staining for Coomassie blue.

RESULTS

The observation that auto-ADP-ribosylated ExoS showed p*I* heterogeneity by 2D SDS−PAGE prompted an analysis to resolve the molecular basis for the heterogeneity. Four forms of ExoS were characterized which included ExoS expressed in the cytoplasm of *P. aeruginosa* (bacterial intracellular ExoS), ExoS secreted through the type III apparatus into the culture medium by *P. aeruginosa* (secreted ExoS), ExoS translocated into eukaryotic cells by the type III apparatus and accessory proteins (PopB, PopD, and PcrV) by *P. aeruginosa* (eukaryotic intracellular ExoS), and ExoS that had been transfected into eukaryotic cells (eukaryotic intracellular ExoS).

Bacterial Intracellular ExoS Shows pI Heterogeneity. Under standard 2D SDS−PAGE conditions, bacterial intracellular ExoS focused at a p*I* of 4 or less, which differs from its predicted p*I* of 5.6 (Figure 2A). Addition of CHAPS to 10% to the IEF components of the analysis improved the yield and resolution of bacterial intracellular ExoS, which focused into four p*I* forms at 5.3, 5.5, 5.7, and 5.9 (Figure 2B). This suggested that within the bacterial cell ExoS was associated with other cellular components that were disrupted by detergent and that the p*I* heterogeneity of ExoS was present prior to secretion or translocation through the type III apparatus.

ExoS Secreted into Culture Media Focuses with pI Heterogeneity. The ability of 10% CHAPS to increase the

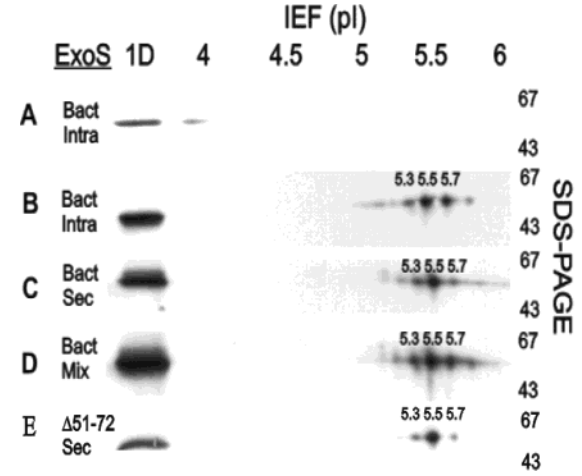

FIGURE 2: Analysis of bacterial intracellular and secreted ExoS by 2D SDS−PAGE. Fifty nanograms of ExoS isolated from bacterial lysates (intracellular, soluble fraction) and focused in the presence of (A) 2% CHAPS or (B) 10% CHAPS or (C) isolated from culture supernatants of *P. aeruginosa* was applied to 2D SDS−PAGE followed by anti-HA Western analysis. (D) A mixture of 50 ng of bacterial intracellular and secreted ExoS was focused as in panels A−C. Densitometry values of the 5.3, 5.5, and 5.7 p*I* forms for bacterial intracellular and secreted ExoS were 5.3 = 18.9 ± 1.0, 5.5 = 49.8 ± 4.0, 5.7 = 31.3 ± 5.1 and 5.3 = 32.8 ± 3.7, 5.5 = 50.6 ± 1.1, 5.7 = 16.6 ± 2.7, respectively. These values represent the mean and standard deviation from three independent determinations. Typically, 60−70% of the starting material (see 1D lane) is recovered following IEF. At an OD_{540} of 4, approximately 40% of the total ExoS present is secreted, 40% is in the soluble fraction, and 20% is in the pellet fraction after high-speed centrifugation following lysis. (E) HA Western analysis of ExoSΔ51−72 showing the same p*I* forms as that of the secreted full-length molecule. Shown are blots from one of four representative experiments.

ability to focus bacterial intracellular ExoS was compared to the p*I* properties of ExoS that had been secreted through the type III apparatus into the culture medium by *P. aeruginosa*. 2D SDS−PAGE of secreted ExoS also focused as four p*I* forms at 5.1, 5.3, 5.5, and 5.7, a pattern similar to the pattern of bacterial intracellular ExoS (Figure 2B,C). A mixing experiment showed that p*I* forms observed for bacterial intracellular ExoS overlapped with secreted ExoS (Figure 2D). The forms that focused at a p*I* of 5.3, 5.5, and 5.7 showed a slight shift in the amount of ExoS that focused at 5.3 relative to the form that focused at 5.7 upon secretion through the type III apparatus, indicating that charge modifications persist on ExoS upon secretion through the type III apparatus.

ExoSΔ51−72 as a Reagent To Study pI Heterogeneity. Type III secreted ExoS forms a molecular complex with a mass greater than 300 kDa (*29*). In contrast, ExoSΔ51−72 behaved as a monomer in solution with an apparent mass of 46 kDa by analytical ultracentrifugation (data not shown), indicating that deletion of amino acids 51−72 eliminates the aggregation of ExoS. Secreted ExoSΔ51−72 focused with a p*I* heterogeneity similar to that of full-length ExoS (Figure 2E). This showed that the p*I* heterogeneity of ExoS is not due to aggregation. Since ExoSΔ51−72 is soluble and can be purified to near homogeneity from *P. aeruginosa*, it was used to analyze the basis for ExoS p*I* heterogeneity.

ExoS pI Heterogeneity Is Not Attributed to a Difference in Mass. To investigate whether the p*I* heterogeneity was due to a posttranslational modification, the five p*I* forms of

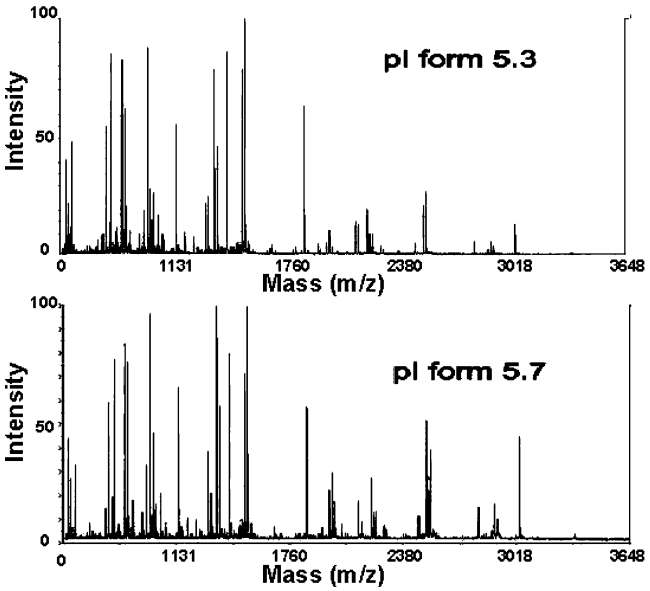

FIGURE 3: Peptide profiles of the 5.3 and 5.7 p*I* forms. Five micrograms of ExoSΔ51−72, purified from culture supernatants of *P. aeruginosa*, was subjected to 2D SDS−PAGE, and the 5.3 and 5.7 p*I* forms were applied to MALDI-MS analysis as described in Experimental Procedures. Shown are representative peptide profiles from trypsin digestion of the 5.3 and 5.7 p*I* forms. The 5.1, 5.5, and 5.9 p*I* forms have identical peptide profiles as the 5.3 and 5.7 forms.

secreted ExoSΔ51−72 (5.1, 5.3, 5.5, 5.7, and 5.9) were subjected to in-gel digestion and MALDI-MS analysis (Figure 3 shows the profiles for the 5.3 and 5.7 forms). Using three proteases, 95% coverage of the primary amino acid sequence of ExoSΔ51−72 was attained. The peptide masses of the four p*I* forms of ExoS were identical, given a sensitivity of less than 1 Da. Table 1 shows the calculated and determined masses for the 5.3 and 5.7 forms of ExoS. Proteolytic processing at the N- or C-terminus was not observed. Peptides not represented in the analysis were too small to be resolved by MALDI-MS and did not contain amino acids modified with known posttranslational modifications. MALDI-MS analysis of secreted ExoSΔ51−72 had a mass of 47527 ± 87 Da, which is similar to a predicted mass of 47508 Da. Taken together, these data indicate that ExoS heterogeneity observed in the IEF system is independent of a mass modification.

The GAP and ADP-Ribosyltransferase Domains Display pI Heterogeneity. To determine if the p*I* heterogeneity was localized to the GAP or ADP-ribosyltransferase domains, ExoS(1−234) (the GAP domain of ExoS, purified from culture supernatants of *P. aeruginosa*) and ExoS(232−453) (the ADP-r domain of ExoS, purified from *E. coli*), were subjected to 2D SDS−PAGE. ExoS(1−234) focused as 6−8 p*I* forms, while ExoS(232−453) formed 8−10 p*I* forms (Figure 4), suggesting that the p*I* heterogeneity was a property within the entire ExoS protein.

pI Heterogeneity Is an Intrinsic Property of ExoS That Represents Native or Partially Native Structural Variants. To determine if the p*I* heterogeneity could be attributed to buffer conditions during IEF, the concentrations of urea (0−10 M), CHAPS (0−10%), and DTT (0−3%) were individually varied, and the ratio of the 5.3, 5.5, and 5.7 p*I* forms of ExoSΔ51−72 (secreted form *P. aeruginosa*) was examined. Focusing ExoSΔ51−72 in 8 M urea without CHAPS, or with

Table 1: Peptide Masses Following Digestion of ExoSΔ51−72 p*I* Forms[a]

peptide	residue no.	calcd mass (MI)	measured mass MI, 5.3	measured mass MI, 5.7
T1	1−23	2522.25	2522.24	2521.57
S1	24−44	2295.56	2294.6	2295.3
T2	31−44	1526.79	1526.80	1526.40
S2	31−82 (Δ51−72)	3143.67	3146.10	3146.31
T3	83−103	2145.06	2145.06	2144.48
T4	104−116	1500.83	1500.81	1500.82
ND	117−120 (GLDK)	359.21	ND	ND
T5	121−134	1428.77	1428.77	1428.00
ND	135−138 (EHSR)	455.2	ND	ND
T6	139−147	859.46	859.24	859.46
T7	148−157	988.58	987.48	987.22
T8	158−166	962.45	962.45	962.21
T9	167−171	544.32	544.30	543.17
T10	172−175	530.33	530.32	530.18
T11	176−204	2896.51	2897.46	2896.50
ND	205 (E)	129.04	ND	ND
T12	206−222	1982.04	1982.05	1982.04
T13	223−231	1004.50	1004.50	1004.24
ND	232−236 (SADK)	347.18	ND	ND
T14	237−244	786.47	786.44	786.25
ND	245 (F)	147.07	ND	ND
T15	246−252	737.35	737.34	737.15
V1	252−266	1627.81	1628.70	1628.00
T16	257−283	2898.42	2897.46	2896.51
V2	267−290	2689.39	2689.70	2690.70
T17	287−296	1073.52	1073.52	1073.24
T18	297−308	1309.65	1309.65	1309.31
T19	309−317	945.50	945.50	945.26
V3	314−333	2164.10	2164.90	2164.30
T20	324−335	1193.54	1193.55	1193.22
T21	336−353	1857.91	1857.90	1857.40
T22	354−366	1356.69	1356.70	1356.34
T23	367−378	1239.62	1239.62	1239.30
ND	379−380 (EK)	239.13	ND	ND
V4	381−388	1036.57	1036.30	1036.64
V5	389−400	1352.63	1352.50	1352.80
T24	393−405	1374.72	1374.72	1374.36
V6	401−409	1039.65	1040.40	1040.70
T25	407−435	3033.55	3033.52	3032.71
T26	436−445	1146.54	1146.54	1146.24
S4	407−448	4430.25	4432.40	4432.30
ND	449−453 (GLDLA)	397.24	ND	ND

[a] The peptide masses after MALDI-TOF analysis of ExoSΔ51−72 are shown for the 5.3 and 5.7 p*I* forms following digestion with either trypsin (T), submaxillaris protease (S), or V8 protease (V). Mass values are in daltons. Sequences not covered by the analysis are indicated in parentheses. MI = monoisotopic; ND = not determined.

10% CHAPS without urea, did not alter the ratio of p*I* forms but lowered the amount of ExoSΔ51−72 that entered the IEF matrix. Varying DTT also did not alter the ratio of p*I* forms (data not shown). As another control to separate the effects of urea from the formation of p*I* heterogeneity, ExoS-(E381D), a form of ExoS catalytically deficient in ADP-ribosyltransferase activity, was delivered into CHO cells using an infection assay and subjected to IEF analysis. ExoS-(E381D) delivered into CHO cells displays five to six p*I* forms (Figure 6A and 7). When focused under various urea conditions, ExoS(E381D) retained the overall pattern of p*I* heterogeneity, while increasing urea facilitated entry into the IEF matrix (Figure 6A). Thus, the ability to form multiple p*I* forms independent of IEF buffer conditions indicates that the charge heterogeneity is a property of ExoS in solution and that CHAPS and urea enhance the ability of the charge forms to interact with the IEF matrix.

The finding that secreted ExoSΔ51−72 did not undergo a mass addition suggested that the p*I* heterogeneity was intrinsic to ExoS. To test this hypothesis, the individual p*I*

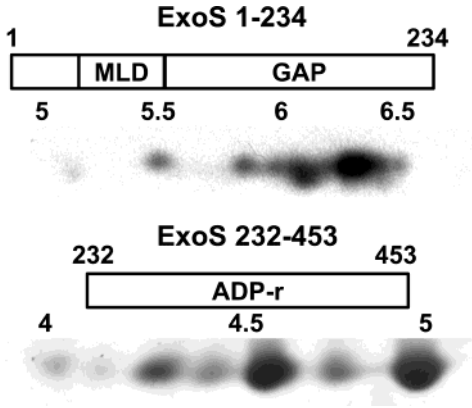

FIGURE 4: Localization of the p*I* heterogeneity to both the GAP and ADPr domains. Fifty nanograms of ExoS(1−234) (GAP domain), secreted from *P. aeruginosa*, and 500 ng of thrombin-cleaved ExoS(232−453) (ADPr domain), purified from *E. coli*, were subjected to 2D SDS−PAGE followed by anti-HA Western and silver staining, respectively. Typically, 6−7 and 7−8 p*I* forms are observed for 1−234 and 232−453, respectively, before resolution is compromised.

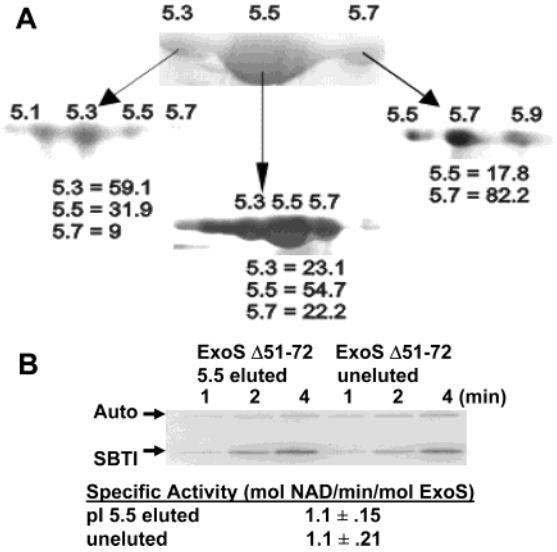

FIGURE 5: Re-2D SDS−PAGE of the 5.3, 5.5, and 5.7 p*I* forms. (A) Fifty micrograms of ExoSΔ51−72, purified from culture supernatants of *P. aeruginosa*, was subjected to 2D SDS−PAGE, and the 5.3, 5.5, and 5.7 p*I* forms were applied to another round of IEF as described in Experimental Procedures. The values were produced by densitometry of the p*I* forms and represent the mean and standard deviation from two independent determinations. Recoveries following elution range from 3% to 15% of the starting material. (B) The 5.5 p*I* form was extracted from an SDS−PAGE gel and assayed for either trans (ribosylation of SBTI) or auto-ADP-ribosyltransferase activity and compared to ExoSΔ51−72 that had not been eluted. Shown is an autoradiogram of 1, 2, and 4 min reactions monitoring the incorporation of [^{32}P]ADP-ribose into substrates. The specific activity was determined by scintillation spectrometry of the excised bands.

forms of ExoSΔ51−72 were isolated and subjected to a second round of 2D SDS−PAGE (Figure 5A). Upon subsequent IEF, each individual p*I* form displayed p*I* heterogeneity with the initial p*I* form being predominant. The 5.3 and 5.7 forms redistributed to more acidic and basic p*I* forms, respectively, suggesting that the p*I* heterogeneity is dynamic and that each form has an intrinsic, but limited, capacity to produce a specific p*I* form.

To determine if the p*I* heterogeneity represented native structural variants, ExoSΔ51−72 was subjected to IEF in

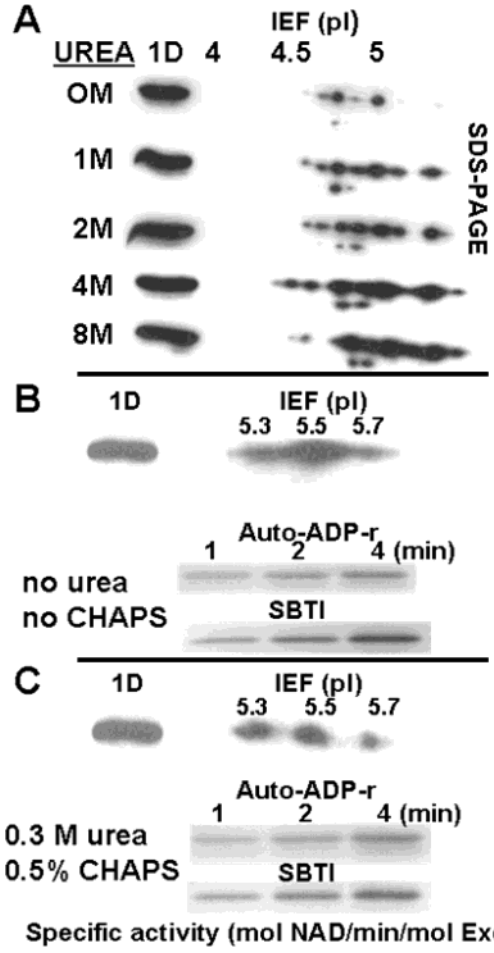

	Auto-ADPr	SBTI
no urea/CHAPS	0.29 ± .03	1.9 ± .14
0.3 M urea,0.5%CHAPS	0.27 ± .04	2.1 ± .35

FIGURE 6: Trans and auto-ADP-ribosylation activity under conditions conducive to formation of p*I* heterogeneity. (A) CHO cells were infected with *P. aeruginosa* expressing ExoS(E381D), and the PNS were isolated and subjected to various urea concentrations during 2D SDS−PAGE followed by HA Western analysis. Each panel is of equal exposure. ExoSΔ51−72, purified from culture supernatants of *P. aeruginosa*, was subjected to IEF in (B) 50 mM Tris, pH 7.6, or (C) 0.3 M urea and 0.5% CHAPS, followed by HA Western analysis. The 5.3, 5.5, and 5.7 p*I* forms are shown for each analysis. The trans and auto-ADP-ribosylation activities were determined as in Figure 5. The specific activity of ExoSΔ51−72 assayed in 0.3 M urea and 0.5% CHAPS was equivalent to that assayed in standard conditions (50 mM Tris, pH 7.6).

the absence of urea or CHAPS. As shown in Figure 6B, ExoSΔ51−72 resolved into the 5.3, 5.5, and 5.7 p*I* forms, with a lower recovery of each p*I* form relative to standard IEF conditions. When focused in 0.3 M urea and 0.5% CHAPS, ExoS formed the 5.3, 5.5, and 5.7 p*I* forms (Figure 6C), which was determined to be the lowest concentration of urea and CHAPS that allowed for maximal resolution and recovery of the p*I* forms. Under conditions conducive to full conformer formation (0.3 M urea, 0.5% CHAPS), ExoSΔ51−72 exhibited trans and auto-ribosyltransferase activity similar to ExoSΔ51−72 assayed in 50 mM Tris, pH 7.6 (Figure 6B,C). The eluted 5.5 p*I* form of ExoS showed trans ADP-ribosyltransferase activity that was similar to native ExoSΔ51−72, which indicated that the eluted material retained catalytic activity (Figure 5B). The 5.3 and 5.7 eluted p*I* forms of ExoS

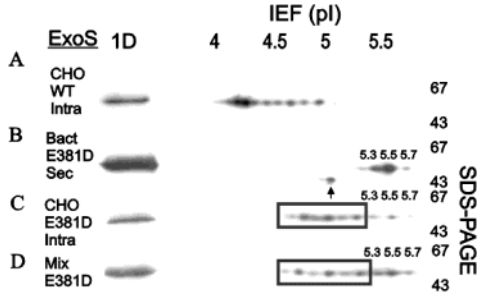

FIGURE 7: Analysis of type III translocated WT ExoS and ExoS(E381D) by 2D SDS−PAGE. CHO cells were infected with *P. aeruginosa* expressing either WT ExoS or ExoS(E381D). Cells were lysed, and proteins were acetone precipitated from postnuclear supernatants (PNS). Ten nanograms of either (A) WT ExoS or (C) ExoS(E381D) was applied to 2D SDS−PAGE followed by anti-HA Western analysis. Sixty percent of ExoS is found in the PNS after a 4 h infection while 40% remains in the pellet after low-speed centrifugation (see Experimental Procedures). ExoS in the pellet shows the same p*I* heterogeneity as that in the PNS. (B) Overexposed anti-HA Western blot of 10 ng of ExoS(E381D) secreted by *P. aeruginosa* to demonstrate the lower p*I* forms are absent as compared to panel C. The arrow indicates a degradation product of ExoS. Sixty percent of the total ExoS(E381D) delivered during a 4 h infection is shifted to lower p*I* forms (boxed area). (D) A mixture of 50 ng of bacterial intracellular and secreted ExoS(E381D).

also showed trans ADP-ribosyltransferase activity similar to ExoSΔ51−72 (data not shown). This indicates that p*I* forms represent native, catalytically active, variants of ExoS.

Eukaryotic Intracellular ExoS(E381D) Possesses pI Heterogeneity That Is Different than Auto-ADP-ribosylated Wild-Type ExoS. ExoS in CHO cells that were infected with *P. aeruginosa* focused as seven to eight p*I* forms with p*I*s between 4.0 and 5.0, more acidic than either bacterial intracellular ExoS or secreted ExoS (Figure 7A). A permeabilization experiment using [^{32}P]NAD showed that each p*I* form was auto-ADP-ribosylated (data not shown). To examine the p*I* heterogeneity of ExoS independent of auto-ADP-ribosylation, the p*I* properties of type III delivered ExoS(E381D) were examined. Previous studies showed that type III delivered ExoS(E381D) was not auto-ADP-ribosylated inside CHO cells (*21*). CHO cells infected with *P. aeruginosa* expressing ExoS(E381D) showed that ExoS(E381D) focused as five unique p*I* forms (p*I*s from ∼4.5 to 5.0) and four p*I* forms similar to secreted ExoS(E381D) (p*I*s ∼5.1−5.7). When compared to bacterial intracellular and type III secreted ExoS(E381D), eukaryotic intracellular ExoS(E381D) focused with p*I* heterogeneity that shifted approximately 0.5 p*I* unit more acidic (Figure 7B,C). A mixture of type III secreted and CHO cell translocated ExoS(E381D) confirmed the negative shift (Figure 7D). Thus, ExoS(E381D) undergoes a negatively charged modification upon type III delivery into eukaryotic cells.

To evaluate if the shift to a lower p*I* was type III dependent, HA-tagged ExoS(R146K,E381D) was transiently transfected into CHO cells and subjected to isoelectric focusing. The Arg146K mutation eliminates ExoS GAP activity, making the protein enzymatically null when expressed in eukaryotic cells. As shown in Figure 8, transfected ExoS(R146K,E381D) focused as five to six major p*I* forms (p*I* ∼4.5−5.2), similar to type III delivered ExoS(E381D). This indicated that ExoS(R146K,E381D) undergoes a negatively charged modification independent of type III delivery.

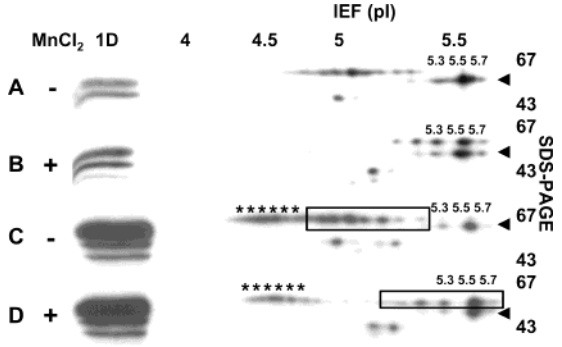

FIGURE 8: $MnCl_2$-dependent p*I* shift of eukaryotic intracellular ExoS(R146K,E381D). Fifty nanograms of transfected ExoS(R146K,-E381D) was incubated with 50 ng of bacterial secreted ExoS-(E381D) alone (A, B) or 50 ng of bacterial secreted ExoS(E381D) and WT ExoS (isolated from an infection assay) (C, D) in the presence (B, D) or absence (A, C) of 0.5 mM $MnCl_2$. Samples were then applied to IEF followed by HA Western analysis. The arrow designates the location of secreted ExoS(E381D). The asterisks denote WT ExoS while the boxed area designates ExoS-(R146K,E381D). The electrophoretic mobility difference observed for WT and transfected ExoS(R146K,E381D) compared to secreted ExoS(E381D) is due to its unique electrophoretic pattern in SDS−PAGE.

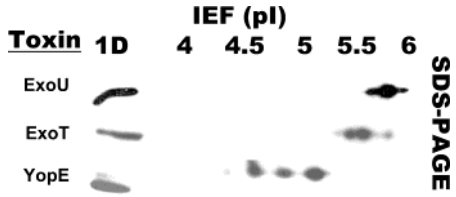

FIGURE 9: p*I* heterogeneity of type III secreted cytotoxins. ExoU, ExoS, and YopE were secreted and isolated from *P. aeruginosa* as described in the legend to Figure 2. ExoU (50 ng) and YopE (50 ng) were subjected to 2D SDS−PAGE (standard conditions), while ExoT (50 ng) was focused in the presence of 10% CHAPS to reduce the amount of protein aggregation. ExoU was detected with the use of an anti-ExoU monoclonal antibody (1:20000), and ExoT and YopE were detected by a HA Western blot as described for ExoS. Representative films of this analysis are shown from one of two independent determinations.

Subsequent analysis showed that 0.5 mM $MnCl_2$ could shift ExoS(R146K,E381D) back to the p*I* of secreted ExoS-(E381D) (Figure 8B). Mammalian ADP-ribosylhydrolases, which remove ADP-ribose moieties in a metal-dependent manner from monoribosylated arginines, have been described (*30*). To determine if the modification to ExoS(K146K,-E381D) was related to auto-ADP-ribosylation, autoribosylated wild-type ExoS isolated from mammalian cells was incubated with transfected ExoS(R146K,E381D) and 0.5 mM $MnCl_2$, followed by IEF and HA Western analysis. While ExoS(R146K,E381D) shifted to a higher p*I* that was identical to that of secreted ExoS(E381D), auto-ADP-ribosylated wild-type ExoS did not undergo a $MnCl_2$-dependent shift in p*I*. This indicated that the $MnCl_2$-dependent shift in p*I* of ExoS-(R146K,E381D) was different than the shift due to auto-ADP-ribosylation of wild-type ExoS.

pI Heterogeneity of Three Type III Cytotoxins, ExoT, ExoU, and YopE. To evaluate if the p*I* heterogeneity was specific to ExoS, three other type III cytotoxins, ExoT and ExoU from *P. aeruginosa* and YopE from *Yersinia pseudotuberculosis*, were subjected to 2D SDS−PAGE analysis. HA Western analysis following IEF/SDS−PAGE showed that each secreted toxin focused with p*I* heterogeneity with three major p*I* forms. ExoU and ExoT distributed in a Gaussian manner near their predicted p*I*s (ExoU, 5.7; ExoT, 5.5) similar to ExoS, whereas YopE was shifted ~1.4 units more negative than its predicted p*I* of 6.4. The reason for this shift in YopE is not known but may be related to its expression or secretion in *P. aeruginosa*.

DISCUSSION

Bacterial intracellular, type III secreted, and type III eukaryotic cell translocated ExoS display p*I* heterogeneity. Using a soluble form of ExoS, ExoSΔ51−72, each p*I* form yielded identical peptide profiles following MALDI-MS analysis. IEF analysis of the GAP and ADPr domains demonstrated each display p*I* heterogeneity, focusing as five or more forms. These data suggest that the p*I* heterogeneity is intrinsic to ExoS, as opposed to being caused by a posttranslational mass modification. The reaction of protonated amino groups on the side chains of arginine and lysine with the urea breakdown product cyanate has been reported during 2D SDS−PAGE (*31*−*33*). To address the possibility that carbamylation was responsible for the p*I* heterogeneity of ExoS, urea was titered into ExoSΔ51−72 and IEF performed. While varying urea from 0 to 10 M (and CHAPS from 0 to 10%) affected the amount of ExoS that entered the IEF matrix, it did not affect the ratio of p*I* forms, suggesting that carbamylation was not responsible for p*I* heterogeneity of ExoS. In addition, boiling ExoSΔ51−72 in 8 M urea did not induce additional p*I* heterogeneity (data not shown). Increasing the amount of urea and CHAPS during focusing increased the amount of the p*I* forms that entered the matrix, suggesting that, although not necessary, either chaotropic agents or detergents contribute to optimal resolution of the observed p*I* heterogeneity. It is possible that urea contributed to the induction of the p*I* heterogeneity of some of the p*I* forms observed in Figure 6A. The p*I* heterogeneity was not dependent on the origin of the protein, as ExoSΔ51−72 purified from either *E. coli* or *P. aeruginosa*, or expressed in eukaryotic cells by transient transfection, showed p*I* heterogeneity. Finally, type III delivered ExoS that did not contain the HA epitope also showed p*I* heterogeneity by IEF (data not shown).

The p*I* heterogeneity of several proteins has been attributed to conformational variants. MALDI-MS analysis indicated that a chemical or posttranslational modification did not account for the multiple isoforms of viscumin, a mistletoe lectin (*28*), or the outer membrane proteins Omp 40 and 41 of *Porphyromonas gingivalis* (*34*). These charge variants form independent of a mass addition or conditions present during focusing and, like ExoS, exist in multiple conformations and thus are defined as conformers. MALDI-TOF analysis of the 5.1, 5.3, 5.5, 5.7, and 5.9 p*I* forms of ExoSΔ51−72 indicated no mass difference in the peptide profiles, given 95% coverage of the primary amino acid sequence. Consistent with the noncovalent and intrinsic nature of the p*I* heterogeneity of ExoS was the determination that isolated conformers of ExoS showed p*I* heterogeneity upon a second round of IEF, where the redistribution of p*I* forms was polarized. The 5.3 form generated more acidic p*I* conformers, and the 5.7 p*I* conformer generated more basic p*I* conformers. This suggests that each p*I* conformer is intrinsically heterogeneous and dynamic, with the potential to distribute into multiple conformers. The observation that

the 5.3 and 5.7 p*I* conformers do not redistribute to the 5.5 p*I* form that is predominant in secreted ExoS suggests that each p*I* conformer may not reach the lowest energy state of the toxin due to the presence of energy barriers among the conformers. Each p*I* form differed from its adjacent p*I* form by 0.1−0.2 unit, a difference consistent with the addition or subtraction of a single negative or positive charge. Thus, the molecular isoforms of ExoS may represent localized changes in the charge distribution of an ionizable group(s) within region(s) of the protein that undergo conformational changes. This differential ionization may be caused by atomic changes in the microenvironment of ExoS, perhaps within regions required for transit through the type III apparatus. The finding that conformers exist under nondenaturing conditions and retain catalytic activity is also consistent with the fact that the charge variants are properties of the native structure of ExoS.

Recent reports indicate that several type III effectors contain coiled-coiled regions that provide a flexible arm for association with components of the translocation apparatus (*35*). The GAP domains of SptP and YopE from *Yersinia* and the ExoS GAP domain contain four-helical bundles that are partially disordered but stabilized upon Rac1 binding, suggesting functional plasticity (*36*, *37*). Recent data also showed that the chaperone binding (Cb) region of YopE is disordered, attaining secondary structure upon SycE (chaperone) binding (*38*). The interaction between chaperone and effector is thought to protect the Cb domain from degradation, as is the case for YopE and SptP (*38*, *39*) and may be true for YopN of *Yersinia* (*40*). These data are consistent with a model whereby effectors translocated through the TTSS contain functional plasticity. Analysis of three other type III cytotoxins, ExoU and ExoT from *P. aeruginosa* and YopE from *Y. pseudotuberculosis*, indicate they also display p*I* heterogeneity. By analogy to ExoS, this finding is consistent with the hypothesis that these toxins exist as charge conformers. Thus, the ability to form conformers may be an intrinsic property of type III proteins and may relate to a common process, such as translocation through the type III apparatus. The dynamic nature of type III cytotoxins during translocation is unknown but may require unfolding and flexibility to transit through the apparatus. A flexible protein in solution may exist in multiple conformational states and, therefore, differentially ionize.

Although most proteins from a eukaryotic cell focus in IEF as a single species, a fair number demonstrate a pattern of p*I* heterogeneity. While the multiple p*I* forms of these proteins may be due to posttranslational modification, it is possible that the p*I* heterogeneity of some of these proteins may be due to noncovalent heterogeneity and related to the ability to attain the flexibility needed to transverse a membrane bilayer. Thus, noncovalent mediated p*I* heterogeneity may be a more common property of proteins than currently appreciated.

The posttranslational modification of toxins and effectors after delivery into eukaryotic cells has been observed. CagA, a type IV secreted cytotoxin from *Helicobacter pylori*, the causative agent of peptic ulcer, is phosphorylated upon translocation into eukaryotic cells (*41*). Tir, a type III secreted effector from enteropathogeneic *E. coli* (EPEC), is phosphorylated on two serines and one tyrosine residue upon delivery into eukaryotic cells. The phosphorylations are believed to induce conformational changes in Tir which facilitate the interaction with the outer membrane protein intimin, which is required for EPEC pedestal formation (*42*, *43*). Attempts to isolate type III translocated ExoS(E381D), either by immunoprecipitation or by the use of narrow p*I* focusing strips, are limited by the amount of ExoS(E381D) delivered in an infection assay, making MALDI-MS analysis not feasible. Type III secreted ExoS(E381D) purified from culture supernatants and incubated with cell lysates does not undergo a shift to a lower p*I* (data not shown), suggesting that the modification is dependent on an intact cellular environment. Using resolving gels, no mobility shift was observed when eukaryotic intracellular ExoS(E381D) was compared to secreted or bacterial intracellular ExoS(E381D), suggesting that the modification, if covalent, is of a low molecular weight. Eukaryotic ExoS(R146K,E381D) can shift back to the p*I* of the secreted and bacterial intracellular ExoS(E381D) in a $MnCl_2$-dependent manner. This conversion is time dependent, and the addition of imidazole and EDTA, chelators of manganese, prevents the $MnCl_2$-dependent shift (A. W. Maresso and J. T. Barbieri, unpublished results). An investigation of the divalent metal dependence in the removal of this negatively charged modification, as well as the characterization of the modification, is currently being carried out in the laboratory.

ACKNOWLEDGMENT

Dr. Darrell McCaslin at the University of Wisconsin's Biophysics Instrumentation Facility performed the analytical ultracentrifugation analysis. We thank Dr. Dara Frank for antisera against ExoU and Dr. Bassam Wakim, Rebecca Krall, Jianjun Sun, Ray Zhang, and Andrew Thill for helpful discussions. MALDI-MS was performed at the Protein−Nucleic Acid Core Facility at the Medical College of Wisconsin.

REFERENCES

1. Adams, C., Morris-Quinn, M., McConnell, F., West, J., Lucey, B., Shortt, C., Cryan, B., Watson, J. B., and O'Gara, F. (1998) *J. Infect. 37*, 151−158.
2. Goehring, U. M., Schmidt, G., Pederson, K. J., Aktories, K., and Barbieri, J. T. (1999) *J. Biol. Chem. 274*, 36369−36372.
3. Coburn, J., Kane, A. V., Feig, L., and Gill, D. M. (1991) *J. Biol. Chem. 266*, 6438−6446.
4. Iglewski, B. H., and Kabat, D. (1975) *Proc. Natl. Acad. Sci. U.S.A. 72*, 2284−2288.
5. Liu, S., Kulich, S. M., and Barbieri, J. T. (1996) *Biochemistry 35*, 2754−2758.
6. Ganesan, A. K., Frank, D. W., Misra, R. P., Schmidt, G., and Barbieri, J. T. (1998) *J. Biol. Chem. 273*, 7332−7337.
7. Riese, M. J., Wittinghofer, A., and Barbieri, J. T. (2001) *Biochemistry 40*, 3289−3294.
8. Barbieri, J. T., Riese, M. J., and Aktories, K. (2002) *Annu. Rev. Cell Dev. Biol. 18*, 315−344.
9. Pederson, K. J., Krall, R., Riese, M. J., and Barbieri, J. T. (2002) *Mol. Microbiol. 46*, 1381−1390.
10. Maresso, A. W., and Barbieri, J. T. (2002) *Protein Expression Purif. 26*, 432−437.
11. Straley, S. C., Skrzypek, E., Plano, G. V., and Bliska, J. B. (1993) *Infect. Immun. 61*, 3105−3110.
12. Kubori, T., Matsushima, Y., Nakamura, D., Uralil, J., Lara-Tejero, M., Sukhan, A., Galan, J. E., and Aizawa, S. I. (1998) *Science 280*, 602−605.
13. Sekiya, K., Ohishi, M., Ogino, T., Tamano, K., Sasakawa, C., and Abe, A. (2001) *Proc. Natl. Acad. Sci. U.S.A. 98*, 11638−11643.
14. Galan, J. E. (2001) *Annu. Rev. Cell Dev. Biol. 17*, 53−86.
15. Page, A. L., and Parsot, C. (2002) *Mol. Microbiol. 46*, 1−11.

16. Bennett, J. C., and Hughes, C. (2000) *Trends Microbiol. 8*, 202−204.
17. Anderson, D. M., and Schneewind, O. (1997) *Science 278*, 1140−1143.
18. Lloyd, S. A., Norman, M., Rosqvist, R., and Wolf-Watz, H. (2001) *Mol. Microbiol. 39*, 520−531.
19. Frithz-Lindsten, E., Holmstrom, A., Jacobsson, L., Soltani, M., Olsson, J., Rosqvist, R., and Forsberg, A. (1998) *Mol. Microbiol. 29*, 1155−1165.
20. Sawa, T., Yahr, T. L., Ohara, M., Kurahashi, K., Gropper, M. A., Wiener-Kronish, J. P., and Frank, D. W. (1999) *Nat. Med. 5*, 392−398.
21. Riese, M. J., Goehring, U. M., Ehrmantraut, M. E., Moss, J., Barbieri, J. T., Aktories, K., and Schmidt, G. (2002) *J. Biol. Chem. 277*, 12082−12088.
22. Kulich, S. M., Frank, D. W., and Barbieri, J. T. (1995) *Infect. Immun. 63*, 1−8.
23. Vallis, A. J., Yahr, T. L., Barbieri, J. T., and Frank, D. W. (1999) *Infect. Immun. 67*, 914−920.
24. Sun, J., and Barbieri, J. T. (2003) *J. Biol. Chem.* (in press).
25. Finck-Barbancon, V., Goranson, J., Zhu, L., Sawa, T., Wiener-Kronish, J. P., Fleiszig, S. M., Wu, C., Mende-Mueller, L., and Frank, D. W. (1997) *Mol. Microbiol. 25*, 547−557.
26. Pederson, K. J., Vallis, A. J., Aktories, K., Frank, D. W., and Barbieri, J. T. (1999) *Mol. Microbiol. 32*, 393−401.
27. Shevchenko, A., Wilm, M., Vorm, O., and Mann, M. (1996) *Anal. Chem. 68*, 850−858.
28. Lutter, P., Meyer, H. E., Langer, M., Witthohn, K., Dormeyer, W., Sickmann, A., and Bluggel, M. (2001) *Electrophoresis 22*, 2888−2897.
29. Kulich, S. M., Frank, D. W., and Barbieri, J. T. (1993) *Infect. Immun. 61*, 307−313.
30. Takada, T., Okazaki, I. J., and Moss, J. (1994) *Mol. Cell. Biochem. 138*, 119−122.
31. Stark, G. R. (1965) *Biochemistry 4*, 2363−2367.
32. Stark, G. R. (1965) *Biochemistry 4*, 1030−1036.
33. King, A. M., and Newman, J. W. (1980) *J. Virol. 34*, 59−66.
34. Veith, P. D., Talbo, G. H., Slakeski, N., and Reynolds, E. C. (2001) *Eur. J. Biochem. 268*, 4748−4757.
35. Delahay, R. M., and Frankel, G. (2002) *Mol. Microbiol. 45*, 905−916.
36. Stebbins, C. E., and Galan, J. E. (2000) *Mol. Cell 6*, 1449−1460.
37. Wurtele, M., Renault, L., Barbieri, J. T., Wittinghofer, A., and Wolf, E. (2001) *FEBS Lett. 491*, 26−29.
38. Birtalan, S. C., Phillips, R. M., and Ghosh, P. (2002) *Mol. Cell 9*, 971−980.
39. Stebbins, C. E., and Galan, J. E. (2001) *Nature 414*, 77−81.
40. Day, J. B., and Plano, G. V. (1998) *Mol. Microbiol. 30*, 777−788.
41. Backert, S., Ziska, E., Brinkmann, V., Zimny-Arndt, U., Fauconnier, A., Jungblut, P. R., Naumann, M., and Meyer, T. F. (2000) *Cell. Microbiol. 2*, 155−164.
42. Kenny, B. (1999) *Mol. Microbiol. 31*, 1229−1241.
43. Warawa, J., and Kenny, B. (2001) *Mol. Microbiol. 42*, 1269−1280.

BI035053I